© 2019. Published by The Company of Biologists Ltd | Development (2019) 146, dev162628. doi:10.1242/dev.162628

RESEARCH REPORT

Defects in efferent duct multiciliogenesis underlie male infertility in GEMC1-, MCIDAS- or CCNO-deficient mice

Berta Terré[1,*], Michael Lewis[1], Gabriel Gil-Gómez[2], Zhiyuan Han[3], Hao Lu[4], Mònica Aguilera[1], Neus Prats[1], Sudipto Roy[4,5,6], Haotian Zhao[3] and Travis H. Stracker[1,‡]

ABSTRACT

GEMC1 and MCIDAS are geminin family proteins that transcriptionally activate E2F4/5-target genes during multiciliogenesis, including *Foxj1* and *Ccno*. Male mice that lacked *Gemc1*, *Mcidas* or *Ccno* were found to be infertile, but the origin of this defect has remained unclear. Here, we show that all three genes are necessary for the generation of functional multiciliated cells in the efferent ducts that are required for spermatozoa to enter the epididymis. In mice that are mutant for *Gemc1*, *Mcidas* or *Ccno*, we observed a similar spectrum of phenotypes, including thinning of the seminiferous tubule epithelia, dilation of the rete testes, sperm agglutinations in the efferent ducts and lack of spermatozoa in the epididymis (azoospermia). These data suggest that defective efferent duct development is the dominant cause of male infertility in these mouse models, and this likely extends to individuals with the ciliopathy reduced generation of multiple motile cilia with mutations in *MCIDAS* and *CCNO*.

KEY WORDS: Fertility, Multiciliated cells, Testes, Efferent ducts, GEMC1, MCIDAS, CCNO, P73, Transcription

INTRODUCTION

Spermatogenesis is a highly regulated developmental process that generates haploid sperm. To become capable of fertilization, spermatozoa must detach from the seminiferous epithelium, enter the tubule lumen and travel through the epididymis, a process that promotes maturation and motility. The efferent ducts (ED) connect the rete testes to the epididymis and are important for sperm concentration, reabsorbing most of the luminal seminiferous fluid (Clulow et al., 1998). The ED epithelia contain poorly characterized multiciliated cells (MCCs) that mobilize luminal fluids through the action of hundreds of motile cilia on the apical surface of these cells (Joseph et al., 2011). The luminal turbulence that is generated by the MCCs of the ED has been proposed to prevent the agglutination of spermatozoa and promote fluid reabsorption by non-MCCs in the ED (Yuan et al., 2019).

[1]Institute for Research in Biomedicine (IRB Barcelona), The Barcelona Institute of Science and Technology, Barcelona 08028, Spain. [2]Apoptosis Signalling Group, IMIM (Institut Hospital del Mar d'Investigacions Mèdiques), Barcelona 08003, Spain. [3]Department of Biomedical Sciences, New York Institute of Technology College of Osteopathic Medicine, Old Westbury, New York, NY 11568, USA. [4]Institute of Molecular and Cell Biology, Proteos, 61 Biopolis Drive, Singapore 138673, Singapore. [5]Department of Pediatrics, Yong Loo Lin School of Medicine, National University of Singapore, 1E Kent Ridge Road, Singapore 119288, Singapore. [6]Department of Biological Sciences, National University of Singapore, 14 Science Drive 4, Singapore 117543, Singapore.
*Present address: The Francis Crick Institute, 1 Midland Road, London NW1 1AT, UK.

‡Author for correspondence (travis.stracker@irbbarcelona.org)

B.T., 0000-0002-0382-6129; G.G.-G., 0000-0002-9790-7308; M.A., 0000-0003-0763-7947; H.Z., 0000-0003-2315-8452; T.H.S., 0000-0002-8650-2081

Received 1 February 2018; Accepted 25 March 2019

Differentiation of airway MCCs is initiated in part through the action of the miR-449/34 family of miRNAs that downregulate numerous genes, including *Cp110* (*Ccp110*), an inhibitor of cilia assembly, as well as Notch genes and *Dll1*, that together inhibit MCC differentiation (Kyrousi et al., 2015; Lafkas et al., 2015; Marcet et al., 2011; Song et al., 2014; Tsao et al., 2009; Zhou et al., 2015). This is followed by the activation of a transcriptional program by the geminin family members GEMC1 (also known as GMNC) and MCIDAS that interact with E2F4/5-DP1 and are required for the generation of MCCs in fish, frogs and mammals (Arbi et al., 2016; Balestrini et al., 2010; Boon et al., 2014; Chong et al., 2018; Danielian et al., 2007; Kyrousi et al., 2015; Lu et al., 2019; Ma et al., 2014; Stubbs et al., 2012; Terré et al., 2016; Zhou et al., 2015). In addition, the transcription factors MYB (Pan et al., 2014; Tan et al., 2013), FOXJ1 (You et al., 2004; Yu et al., 2008), RFX2/3 (Chung et al., 2012; Didon et al., 2013; El Zein et al., 2009) and TAp73 (transcriptionally active isoform encoded by the *Trp73* gene) (Marshall et al., 2016; Nemajerova et al., 2016), as well as the atypical cyclin CCNO (Funk et al., 2015; Núnez-Ollé et al., 2017; Wallmeier et al., 2014), are necessary to promote deuterosome-mediated centriole amplification and the generation of multiple motile cilia. Mutations in *MCIDAS* or *CCNO* underlie reduced generation of multiple motile cilia (RGMC), a rare ciliopathy that is characterized by hydrocephalus, mucus accumulation in the respiratory system and reduced fertility, all presumably due to defects in MCC differentiation (Amirav et al., 2016; Boon et al., 2014; Funk et al., 2015; Wallmeier et al., 2014).

Male and female infertility occurs in a number of mice that are mutant for genes involved in MCC development, including *Ccno*, the miR-34b/c and miR-449a/b/c (miR-dKO) loci, *Trp73*, *E2f4/5*, *Mcidas* and *Gemc1*. When this has been addressed in females, it appears to be because of the loss of MCCs in the oviducts (Chen et al., 1998; Lu et al., 2019; Marshall et al., 2016; Núnez-Ollé et al., 2017; Terré et al., 2016; Wu et al., 2014). However, in males, the origin of the defect has not been clearly established in all cases. Both miR-34/449 and *Trp73* are expressed in the testes, and miR-dKO mice are impaired in meiosis and spermiogenesis and exhibit a 'nearly empty' seminiferous tubule phenotype (Comazzetto et al., 2014; Holembowski et al., 2014; Wu et al., 2014; Yuan et al., 2015). *Trp73*-deficient mice showed a similar seminiferous tubule phenotype (Tomasini et al., 2008), as well as degeneration of the Sertoli cells (SCs) that support spermatid development and ensure integrity of the blood-testes barrier (Holembowski et al., 2014). However, a conditional knockout of 3 out of 4 *E2f4* and *E2f5* alleles in the EDs, but not spermatogonia or spermatocytes, as well as the *Foxj1*-Cre (MCC specific) mediated miR-dKO deletion, phenocopied the seminiferous tubule phenotype (Danielian et al., 2016; Yuan et al., 2019). This indicates that ED defects, particularly in the MCC population, are likely to be sufficient to cause testicular atrophy and male infertility.

Development (2019) 146, dev162628. doi:10.1242/dev.162628

Here, we show that male mice lacking *Gemc1*, *Mcidas* or *Ccno* exhibited a testes phenotype similar to miR-dKO, *Trp73* deletion or loss of multiple *E2f4* and *E2f5* alleles (Comazzetto et al., 2014; Danielian et al., 2016; Holembowski et al., 2014; Inoue et al., 2014; Terré et al., 2016; Wu et al., 2014; Yuan et al., 2015). We found that *Gemc1*-, *Mcidas*- or *Ccno*-deficient mice exhibited luminal dilation of the seminiferous tubules, atrophy of the germinal epithelium, rete testes dilation, SC degeneration and failure of spermatozoa to enter the epididymis, instead accumulating in the EDs. In each case, defects in MCC maturation were clearly evident. Moreover, we show that, similar to *Foxj1*, *Trp73* expression is high in the EDs and is dependent on GEMC1 but not on MCIDAS or CCNO, further establishing the distinct temporal roles of these factors. Our results demonstrate that GEMC1, MCIDAS and CCNO are required for ED MCC differentiation, and this further underscores that these defects are likely to be the primary cause of male infertility in several mouse lines with MCC defects, and potentially in human RGMC patients with mutations in *MCIDAS* or *CCNO*.

RESULTS AND DISCUSSION

GEMC1 loss impairs the late stages of spermatogenesis

We analyzed adult testes of *Gemc1*$^{-/-}$ mice over the first three months and found no consistent changes in size and weight compared with wild-type (Wt) or *Gemc1*$^{+/-}$ littermates when normalized to body size (Fig. 1A). Histological evaluation during the first semi-synchronous wave of spermatogenesis revealed no overt differences between Wt, *Gemc1*$^{+/-}$ or *Gemc1*$^{-/-}$ testes during the first 20 days post partum (p0-p20) (Fig. 1B,C). However, by p27-p35, the thinning of the seminiferous germinal epithelia became obvious, corresponding to the first appearance of elongating spermatids (ES) (Fig. 1B,D). Despite the reduction in cellularity, numbers of mitotic cells, dead cells, meiotic progression and levels of hormonal gene expression were normal in *Gemc1*$^{-/-}$ mice (Fig. S1A-E).

Consistent with histological observations, *Gemc1* messenger RNA (mRNA) expression peaked around p27, although peak levels were considerably lower than in the trachea, which contains a large number of MCCs (Fig. 1E,F). As the peak of *Gemc1* expression and appearance of seminiferous tubule dilation correlated with late stages of spermatogenesis (Fig. 1E), we isolated and quantified enriched populations of testicular cell types [leptotene-zygotene (LZ), pachytene-diplotene (PD), round spermatids (RS) and ES] by fluorescence-activated cell sorting (FACS) (Fig. S1F). *Gemc1* mRNA was enriched in RS and ES populations compared with the germ cell pellet (Fig. 1G) and a significant reduction in RS and ES populations was observed in testes from *Gemc1*$^{-/-}$ mice (Fig. 1H), compared with similar numbers of prophase cells (LZ and PD). This suggested that GEMC1 may support late stages of spermatogenesis through the control of transcription, but the prominent role of GEMC1 in MCC differentiation and the phenotypic similarity to miR-dKO mice prompted us to consider that these effects may be secondary to defects in MCC function in the EDs (Comazzetto et al., 2014; Yuan et al., 2019).

Hypocellularity and dilation of the seminiferous tubules and rete testes

In conditional *E2f4*$^{-/-}$ *E2f5*$^{+/-}$ or miR-dKO mice generated with Cre transgenes active in the EDs of the epididymis and not the testes, defects in MCC formation in the EDs and signs of fluid backpressure, namely seminiferous tubule and rete testes dilation, have been described (Danielian et al., 2016; Yuan et al., 2019). We examined the transcriptional activation of GEMC1 target genes in the testes and, in contrast to tissues containing MCCs, we did not observe any significant alterations in *Ccno*, *Mcidas*, *Foxj1*, *Trp73* and *Cdc20b* in the absence of GEMC1 (Fig. 2A). This was further confirmed at the protein level for TP73 (Fig. 2B). As male mice that are mutant for *Mcidas* and *Ccno*, which, like GEMC1, play key roles in MCC development, were also infertile (Lu et al., 2019; Núnez-Ollé et al., 2017), we histologically examined the testes of these animals in parallel to *Gemc1*$^{-/-}$. In each case they exhibited a similar seminiferous tubule phenotype characterized by reduced cellularity and luminal dilation (Fig. 2C,D). Moreover, extensive rete testes dilation was apparent (Fig. 2E), indicative of fluid backpressure.

Previous work has reported seminiferous tubule dilation accompanied by extensive SC degeneration and spermatid detachment due to loss of *Trp73*, which is also required for MCC generation (Holembowski et al., 2014; Inoue et al., 2014; Marshall et al., 2016; Nemajerova et al., 2016; Tomasini et al., 2008). Immunostaining of vimentin-containing intermediate filaments, one of the main components of the SC cytoskeleton (Aumüller et al., 1988), revealed marked structural abnormalities in the SCs of *Gemc1*-, *Mcidas*- and *Ccno*-deficient testes (Fig. 2F,G). This was characterized by abnormally shorter and thinner cytoplasmic projections and the appearance of SC-only seminiferous tubules (Fig. 2H) and was accompanied by extensive spermatid detachment in *Gemc1*$^{-/-}$ mice (Fig. 2I). In contrast, the SCs of Wt mice extended long cytoplasmic arms in contact with germ cell populations (Fig. 2F, G,I). Thus, *Gemc1*, *Mcidas* and *Ccno* mutants phenocopied the loss of *Trp73*, *E2f4/5* and miR-dKO, exhibiting dilated seminiferous tubules and SC degeneration, with the loss of GEMC1 having little impact on the expression of known MCC transcriptional targets in the testes.

Defective movement of spermatozoa to the epididymis in *Gemc1*$^{-/-}$, *Mcidas*$^{-/-}$ and *Ccno*$^{-/-}$ mice

Spermatozoa enter the caput epididymis but remain immature until reaching the cauda epididymis, where they acquire motility and fertilization competency (Fig. 3A). *Gemc1*$^{-/-}$ and *Ccno*$^{-/-}$ epididymides appeared to be paler, smaller and thinner than Wt (Fig. 3B). Histological analysis of *Gemc1*$^{-/-}$, *Mcidas*$^{-/-}$ and *Ccno*$^{-/-}$ revealed no detectable sperm in the caput, corpus or cauda epididymides in any case, in contrast to Wt, in which sperm were abundant in all sections (Fig. 3C). Consistent with this, the lumen of *Gemc1*$^{-/-}$, *Mcidas*$^{-/-}$ and *Ccno*$^{-/-}$ epididymides was often filled with amorphous periodic acid–Schiff stain (PAS)-positive material, a phenotype that is typically observed in the absence of spermatozoa (Abe and Takano, 1988). *Gemc1*$^{-/-}$, *Mcidas*$^{-/-}$ and *Ccno*$^{-/-}$ males thus have an apparently complete block in transit of spermatozoa to the epididymis.

As the EDs are crucial for sperm transit and contain MCCs, we examined *Gemc1*, *Mcidas* and *Ccno* expression in the testes, cauda epididymis and EDs. The expression of *Gemc1* was considerably higher in the EDs than in testes (Fig. 3D), and similar to its levels in the trachea. A similar pattern was observed for its target gene *Mcidas* (Fig. 3E), as well as *Trp73* (Fig. 3F). In contrast, *Ccno* was marginally upregulated in the ED compared with the testes and further increased in the cauda epididymis (Fig. 3G), suggesting that it may play roles independently of GEMC1 and MCIDAS, which both appear to be restricted to MCCs in other tissues (Kyrousi et al., 2015).

We next examined the expression levels of key MCC regulators in *Gemc1*$^{-/-}$ EDs. Although *Ccno* levels were moderately increased, other known target genes including *Mcidas*, *Cdc20B* and *Foxj1*, as well as *Trp73*, were strongly downregulated (Fig. 3H), consistent

Development (2019) 146, dev162628. doi:10.1242/dev.162628

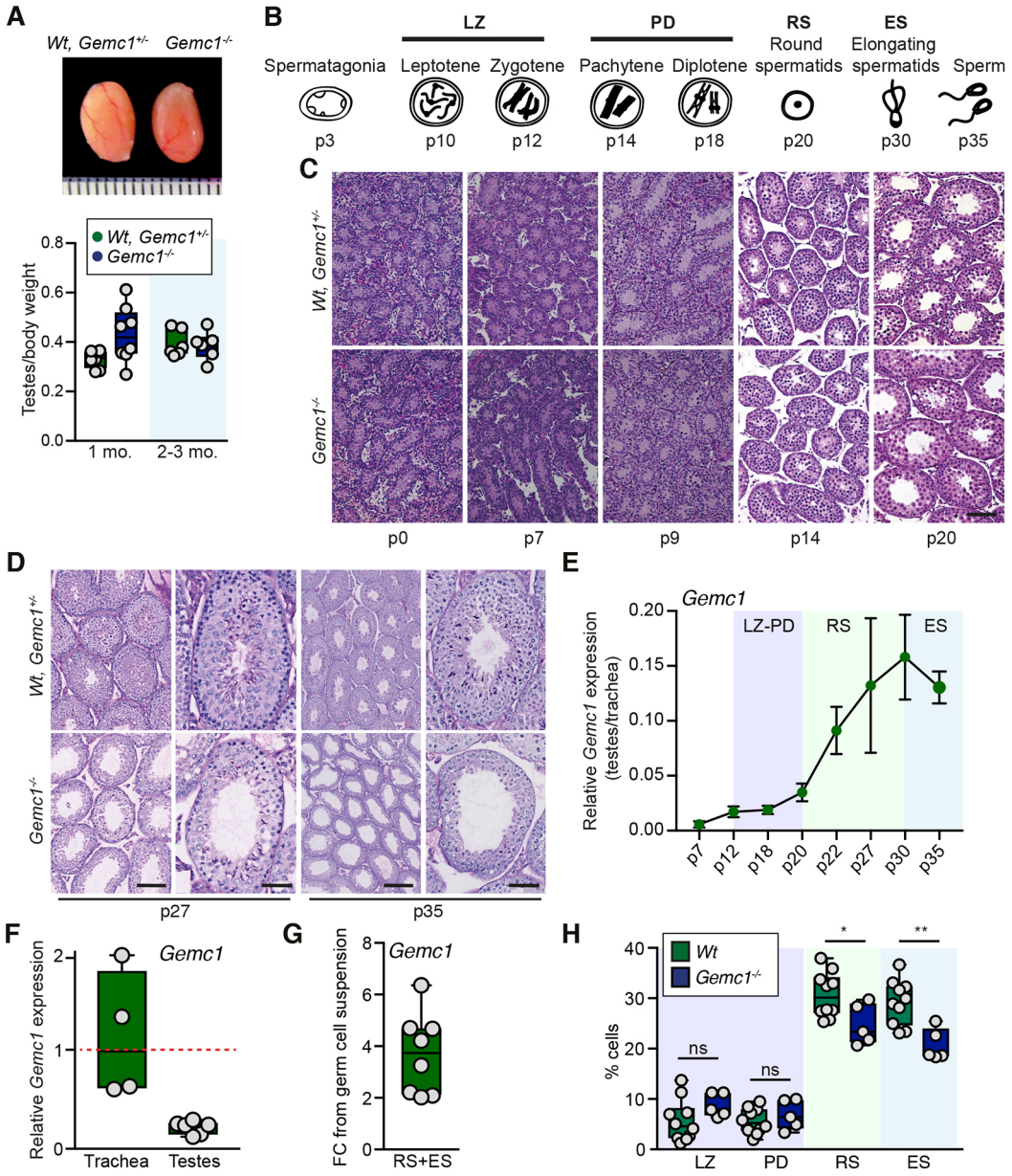

Fig. 1. *Gemc1* loss impairs late stages of spermatogenesis. (A) Example of testes from littermate mice of the indicated genotypes at 3 months (top). Ruler: mm. Testes weight relative to whole body weight at the indicated ages (n=8 for 1 month and n=6 animals/genotype for 2-3 months) (bottom). (B) Schematic of semi-synchronous stages of spermatogenesis in mice (adapted from Comazzetto et al., 2014). (C) PAS staining of developing testes from Wt, *Gemc1*$^{+/-}$ and *Gemc1*$^{-/-}$ littermates at p0, p7, p9, p14 and p20. Scale bar: 100 µm. (D) PAS staining of p27 and p35 testes. Note thinner seminiferous tubule epithelia in *Gemc1*$^{-/-}$. Scale bars: 200 µm (p27, p35: left panels); 50 µm (p27, p35: right panels). (E) RT-qPCR analysis of *Gemc1* expression in testes at the indicated post partum days (n=2 animals for p7, p18, p20, p30; n=3 animals for p12, p22, p27, p35) and plotted relative to the trachea. *Actb* was used as a normalization control. Data are mean±s.d. (F) RT-qPCR analysis of *Gemc1* expression in 1- to 2-month-old testes (n=6) compared with trachea (n=4). *Actb* was used as a normalization control. (G) Ratio of *Gemc1* expression in isolated RS/ES populations compared with germ cell pellets (RT-qPCR, n=8 animals). *Actb* was used as a normalization control. (H) Comparative abundance of each spermatogenic cell type of control and *Gemc1*$^{-/-}$ mice using FACS (Wt, n=10 animals; *Gemc1*$^{-/-}$, n=5 animals). Box and whisker plots (A,F-H): median values (middle bars) and first to third interquartile ranges (boxes); whiskers indicate min to max; dots indicate data points. *P=0.023 and **P=0.0023, unpaired two-tailed t-test. ns, not significant; p, post partum days.

with what has been observed in the trachea (Terré et al., 2016). Similar to what has been reported for miR-dKO, or *Trp73*- and *E2f4/5*-deficient mice, PAS staining of histological sections revealed sperm agglutinations in the EDs of *Gemc1*$^{-/-}$, *Mcidas*$^{-/-}$ and *Ccno*$^{-/-}$ mice; they are normally not detected in Wt animals because of the rapid transit through this region (Fig. 3I). Therefore, regardless of gene expression patterns in the testes, spermatozoa were unable to enter the epididymis of *Gemc1*$^{-/-}$, *Mcidas*$^{-/-}$ and *Ccno*$^{-/-}$ males, corresponding with defects in ED formation or function. In the case of GEMC1, this appeared to reflect its transcriptional role, similar to other MCC-containing tissues.

Distinct temporal roles of GEMC1, MCIDAS and CCNO in the EDs

Staining of motile cilia with anti-acetylated tubulin (ac-tub) antibodies revealed that columnar MCCs were absent in *Gemc1*$^{-/-}$ EDs (Fig. 4A). A less severe phenotype was observed in both *Mcidas*$^{-/-}$ and *Ccno*$^{-/-}$ mice, as some cells with MCC morphology

Development (2019) 146, dev162628. doi:10.1242/dev.162628

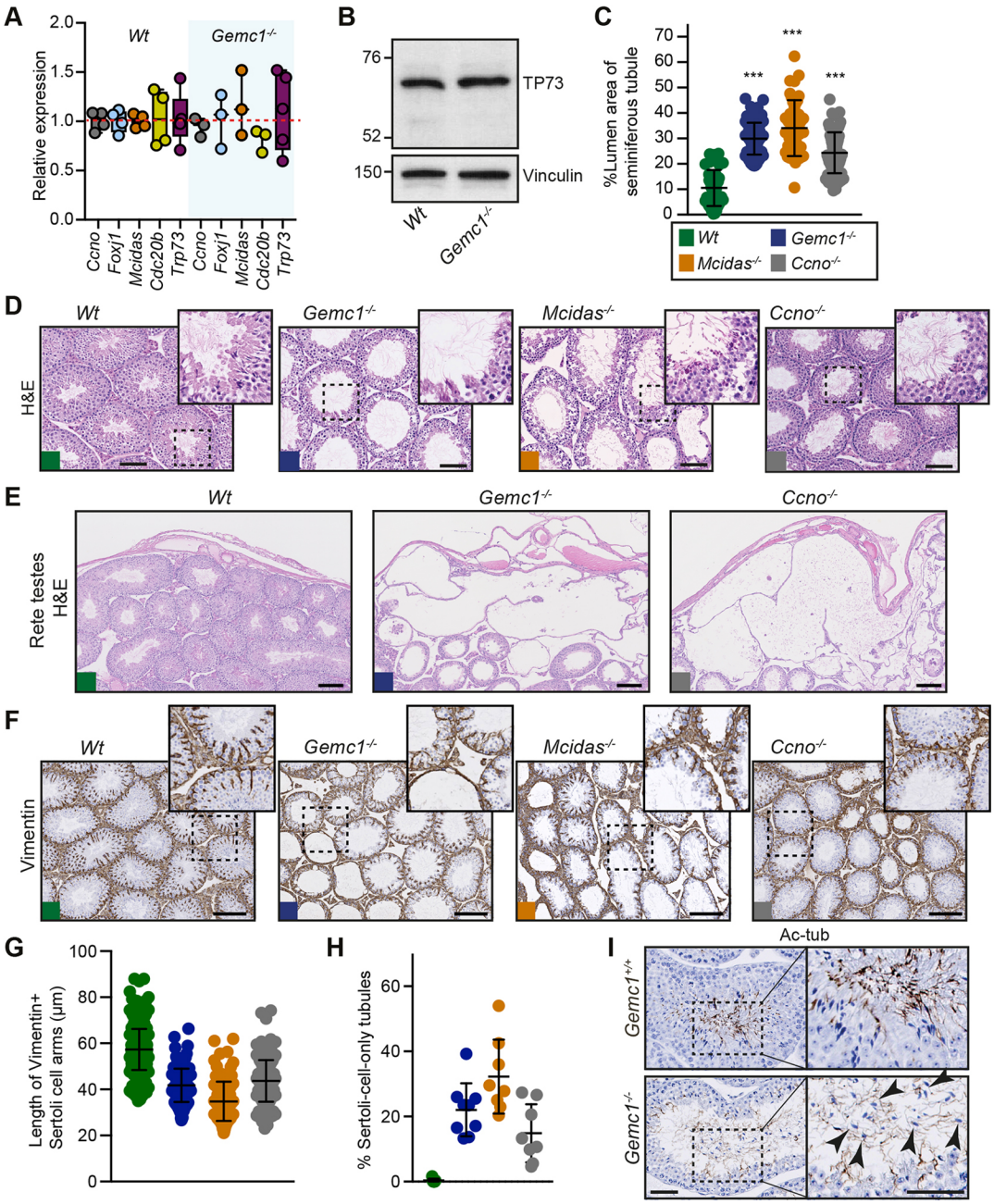

Fig. 2. Seminiferous tubule and rete testes dilation and SC degeneration in testes of *Gemc1*, *Mcidas* or *Ccno* mutant mice. (A) RT-qPCR analysis of *Ccno*, *Mcidas*, *Foxj1*, *Trp73* and *Cdc20b* in the p27 testes of Wt (n=4) and *Gemc1*$^{-/-}$ (n=3) mice. For *Trp73* n=5 for both genotypes. *Actb* was used as a normalization control. (B) A representative western blot of TP73 levels in testes lysates from p27 Wt or *Gemc1*$^{-/-}$ (n=2). Vinculin was used as a loading control. (C) Quantification of empty lumen space (n=4 testes/genotype). (D) H&E staining of testes sections from p35-p37 *Gemc1*$^{-/-}$, *Mcidas*$^{-/-}$ and *Ccno*$^{-/-}$ mice revealed thinning of the spermatogenic cell layer. (E) Examples of rete testes dilation in the indicated genotypes at p35. (F) Vimentin staining of SC intermediate filaments in the testes of the indicated genotype. (G) Quantification of the length of vimentin-positive SC arms (Wt, n=4; *Gemc1*$^{-/-}$, *Mcidas*$^{-/-}$ and *Ccno*$^{-/-}$, n=2 animals/genotype). Genotype key as in C. (H) SC-only tubules (n=4 testes/genotype). Results from p30-37 testes are shown. Genotype key as in C. (I) Ac-tub staining of p35 seminiferous tubules of Wt (*Gemc1*$^{+/+}$) and *Gemc1*$^{-/-}$ mice. Detached spermatids in *Gemc1*$^{-/-}$ indicated by black arrowheads. Data are mean±s.d.; dots indicate data points. ***P<0.0001, unpaired two-tailed t-test. Insets show magnification of boxed areas. Scale bars: 100 µm in D,F; 200 µm in E; 50 µm in I.

were apparent, but few cilia visible (Fig. 4A). In all three mutants, ac-tub staining was observed in spermatozoa agglutinations in the central cavity of the ED.

The ED epithelium of *Gemc1*$^{-/-}$ mice was thinner than that of Wt, *Mcidas*$^{-/-}$ and *Ccno*$^{-/-}$ mice (Fig. 4A), so we examined the expression of the FOXJ1 and TP73 transcription factors that are crucial for MCC formation in other tissues (Marshall et al., 2016; Nemajerova et al., 2016; You et al., 2004). Cells lining the EDs were strongly immunopositive for FOXJ1 in Wt and *Ccno*$^{-/-}$, but staining was completely absent in *Gemc1*$^{-/-}$ (Fig. S2A). Similarly, TP73-positive cells were absent in *Gemc1*$^{-/-}$, but readily identifiable in both *Mcidas*$^{-/-}$ and *Ccno*$^{-/-}$ mice (Fig. 4B). We, and others, have previously shown that the transient transfection of GEMC1 can activate early MCC factors, including both *MCIDAS* and *FOXJ1*, in AD293 cells (Arbi et al., 2016; Lu et al., 2019; Terré et al., 2016). Transient overexpression of GEMC1 led to a strong

Development (2019) 146, dev162628. doi:10.1242/dev.162628

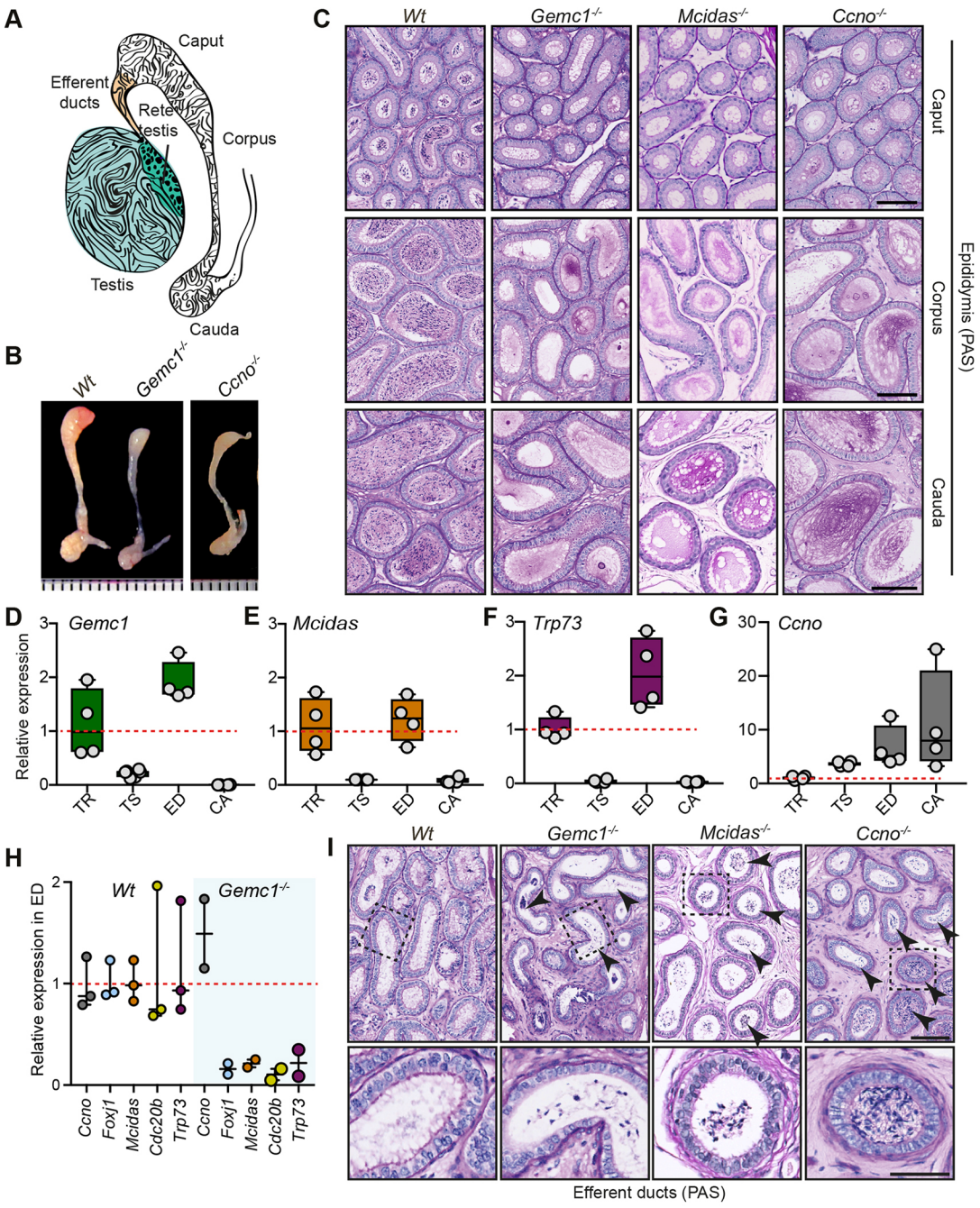

Fig. 3. *Gemc1*, *Mcidas* or *Ccno* deficiency causes sperm agglutination in the ED. (A) Schematic of a vertical section of the testis, rete testis, EDs and epididymis (caput, corpus, cauda). (B) Gross morphology of the p35-p37 epididymides of the indicated genotypes. Ruler: mm. (C) PAS staining of the three major regions of the mouse epididymis (caput, corpus and cauda) from adult mice of the indicated genotype. (D-G) RT-qPCR analysis of the expression levels of the indicated gene in different tissues (TR, trachea; TS, testes; ED, efferent ducts; CA, cauda epididymis), normalized to the trachea (n=4 p35 animals). *Actb* was used as a normalization control. Red dashed line indicates normalized average in the TR. Box and whisker plots: median values (middle bars) and first to third interquartile ranges (boxes); whiskers indicate min to max; dots indicate data points. (H) RT-qPCR analysis of the expression levels of the indicated gene in the EDs of p35 Wt (n=3) or *Gemc1*$^{-/-}$ (n=2) animals. *Actb* was used as a normalization control. Data are mean±s.d.; dots indicate data points. (I) PAS staining of the p35-p37 EDs of mice of the indicated genotype. Black arrowheads indicate the aberrant accumulation of spermatozoa in the *Gemc1*$^{-/-}$ and *Ccno*$^{-/-}$ mice compared with Wt. Bottom panels show magnification of boxed areas. Scale bars: 100 µm in C,I (top panels); 50 µm in I (bottom panels).

increase in *Trp73* mRNA and protein levels, in contrast to CCNO overexpression that did not influence its levels (Fig. 4C), demonstrating that GEMC1 can activate TP73 expression.

Collectively, our experiments demonstrated that male mice lacking *Gemc1*, *Mcidas* or *Ccno* were infertile and exhibited a testes phenotype closely resembling that of *Trp73*-deficient mice, or ED-specific miR-dKO or *E2f4*$^{-/-}$*E2f5*$^{+/-}$ deletions (Comazzetto et al., 2014; Holembowski et al., 2014; Yuan et al., 2019). The impairment of the MCC transcriptional program and agglutination of spermatozoa in the EDs appears to be sufficient to generate backpressure that prevents spermatozoa from entering the epididymis (Yuan et al., 2019). We propose that impaired MCC function is likely the dominant cause of infertility in *Gemc1*$^{-/-}$, *Mcidas*$^{-/-}$ and *Ccno*$^{-/-}$ mice, and potentially in male RGMC

Development (2019) 146, dev162628. doi:10.1242/dev.162628

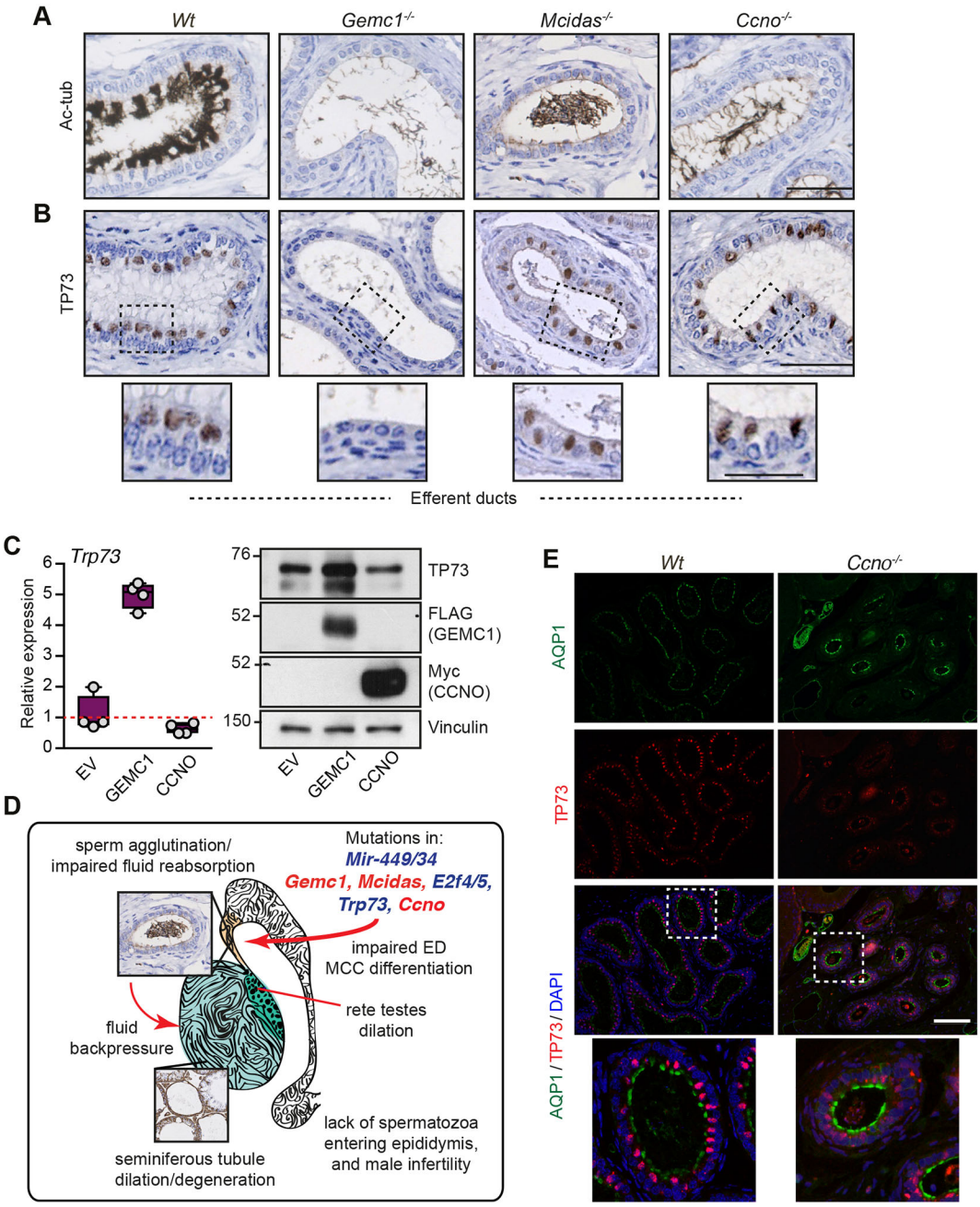

Fig. 4. GEMC1, MCIDAS and CCNO are required for ED MCC development. (A) Representative ac-tub staining of p35-p37 EDs of the indicated genotypes. (B) ED sections of the indicated genotypes stained with an antibody against TP73. (C) Overexpression of FLAG-GEMC1, but not Myc-CCNO, in AD293 cells by transient transfection induces TP73 expression. RT-qPCR was used to measure relative mRNA levels (n=4) and a representative western blot of three independent experiments is shown. *Actb* was used as a normalization control and vinculin as a loading control for western blots. (D) Mice with mutations in miR-449/34, *Gemc1*, *Mcidas*, *E2f4*/*5*, *Trp73* and *Ccno* exhibit defects in MCC development and a similar phenotypic spectrum that includes dilation of the seminiferous tubules and rete testes, SC degeneration and lack of spermatozoa in the epididymis (azoospermia). We propose that the failure of the EDs and resulting agglutination of spermatozoa contributes directly to fluid backpressure, preventing spermatozoa from entering the epididymis. This potentially occurs in human RGMC patients with *MCIDAS* or *CCNO* mutations. (E) Immunofluorescent co-immunostaining of AQP1 and TP73 in EDs of p30-35 animals of the indicated genotypes. Insets show magnification of boxed areas. Scale bars: 100 µm in A,B; 50 µm in B (insets); 200 µm in E.

patients that harbor mutations in *MCIDAS* or *CCNO* (Fig. 4D). The seminiferous tubule and rete testes dilation, degeneration of the SC support structures and failure of spermatozoa to enter the epididymis is most likely a secondary effect of backpressure caused by loss of MCC function that results in the agglutination of spermatozoa in the EDs. We cannot, however, rule out a role for these factors in other cell types of the ED that are associated with reabsorption of seminal vesicle fluids, as has been proposed for both *Esr1* and *E2f4/5* mutants (Danielian et al., 2016; Joseph et al., 2011). However, we observed normal staining of the E2F4/5-dependent AQP1 marker of secretory cells in CCNO and GEMC1 mutants, suggesting that E2F4/5-mediated transcription is not severely affected in non-MCC cell types of the ED in these mice (Fig. 4E and Fig. S2B) (Danielian et al., 2016).

The roles of GEMC1 and MCIDAS in multiciliogenesis are primarily related to transcription and our data lend further support to

Development (2019) 146, dev162628. doi:10.1242/dev.162628

them acting in a stepwise manner, with GEMC1 playing a key role in specification and MCIDAS required for ciliogenesis (Fig. 4B). However, the function of CCNO remains enigmatic. Recent work demonstrated that the mitotic oscillator and fine-tuning of CDK activity is required for stepwise deuterosome-mediated centriole amplification in MCCs (Al Jord et al., 2017; Vladar et al., 2018). Given that CCNO interacts with CDK1 and CDK2 (Roig et al., 2009), and CCNO-deficient mice exhibit abnormal deuterosomes (Funk et al., 2015), it appears plausible that one of its primary functions is CDK regulation during deuterosome formation. Future work will be needed to understand precisely how GEMC1, MCIDAS and CCNO regulate different aspects of the transcriptional response and deuterosome formation, as well as their potential roles in other tissues.

MATERIALS AND METHODS

Histopathology and immunohistochemistry of murine tissues

Gemc1$^{-/-}$, *Mcidas*$^{-/-}$ and *Ccno*$^{-/-}$ mice on a mixed C57BL/6-129SvEv background have been described previously (Lu et al., 2019; Núnez-Ollé et al., 2017; Terré et al., 2016). Animals were maintained in accordance with the European Community (86/609/EEC) guidelines in the specific-pathogen free (SPF) facilities of the Barcelona Science Park (PCB) and in SPF facilities following guidelines of the Biological Resource Center of the Agency for Science, Technology and Research (A*STAR) of Singapore. Protocols were approved by the Animal Care and Use Committee of the PCB (IACUC; CEEA-PCB) in accordance with applicable legislation (Law 5/1995/GC; Order 214/1997/GC; Law 1201/2005/SG) and ethical guidelines of the Singapore National Advisory Committee on Laboratory Animal Research. All efforts were made to minimize use and suffering. Sample sizes were not defined to detect pre-determined effect size. Animals were not randomized, were identified by genotyping for analysis and were all males, and ages are indicated in the figure legends.

Testes and epididymis were harvested and fixed in 4% paraformaldehyde (PFA) or Bouin's solution (Electron Microscopy Sciences) overnight at 4°C, dehydrated using a graded series of ethanols, transferred to xylene and embedded in paraffin wax. Sections were cut at 3-5 µm thickness, dewaxed and stained with Hematoxylin and Eosin (H&E) and PAS (Sigma-Aldrich) using a CoverStainer (Dako-Agilent) following the manufacturer's instructions. For immunohistochemistry (IHC), epitope retrieval was performed using citrate pH 6 buffer in an autoclave at 121°C for 12 min. Washings were performed using the Wash Solution AR (AR10211-2, Dako, Agilent). Quenching of endogenous peroxidase was performed by 10 min of incubation with Peroxidase-Blocking Solution at room temperature (RT) (S2023, Dako, Agilent). Non-specific unions were blocked using 5% of goat normal serum (16210064, Life Technologies) mixed with 2.5% bovine serum albumin (BSA) diluted in wash buffer for 60 min at RT. Ac-tub was also blocked with M.O.M.™ Blocking Reagent (MK-2213, Vector Laboratories) following the manufacturer's instructions. IHC was performed using an Autostainer Plus (Dako, Agilent) for p73 antibody (90 min at RT) and manually for ac-tub staining (overnight at 4°C). The secondary antibodies used were a BrightVision poly-HRP-anti-rabbit IgG biotin-free (DPVR-110HRP, Immunologic), ready to use for 45 min at RT, and a polyclonal goat anti-mouse immunoglobulins/HRP (P0447, Dako) diluted at 1:100 for 30 min at RT. Antigen–antibody complexes were revealed with 3-3′-diaminobenzidine (K346811, Dako), with the same time exposure (10 min). Sections were counterstained with Hematoxylin (CS700, Dako, Agilent) and mounted with toluene-free mounting medium (CS705, Dako, Agilent) using a Dako CoverStainer. Specificity of staining was confirmed by omission of the primary antibody or staining with rabbit IgG, polyclonal-isotype control (ab27478, Abcam) or a mouse IgG-isotype control (ab37355, Abcam). For γH2AX and pH3S10, sections were incubated with primary antibody overnight at room temperature after quenching endogenous peroxidase using 0.6% H_2O_2 (vol/vol) in methanol for 10 minutes. Slides were washed and labeled with the Vectastain Elite kit (PK-6100, Vector Labs) and immunoreactive signals visualized with the VIP substrate kit (SK-4600, Vector Labs) using the manufacturer's protocol. Sections were counterstained with 0.1% (wt/vol) Methyl Green (67060, Merck), dehydrated and mounted in DPX mountant (06522, Merck). Brightfield images were acquired using a NanoZoomer-2.0 HT C9600 digital scanner (Hamamatsu) equipped with a 20× objective. All images were visualized using the NDP.view2 U123888-01 software (Hamamatsu Photonics). All images were visualized with a gamma correction set at 1.8 in the image control panel of the NDP.view2 U12388-01 software. For TUNEL staining, testes sections were labeled with In Situ Cell Death Detection Kit (TUNEL) (11684795910, Roche) according to the manufacturer's instructions.

Antibodies

Primary antibodies used in the publication were: mouse anti-ac-tub (6-11B-1, T6793, Sigma-Aldrich, 1:1000); rabbit anti-vimentin (EPR3776, ab92547, Abcam, 1:2000); rabbit anti-vinculin (EPR8185, ab129002, Abcam, 1:2000); rabbit anti-TP73 (EP436Y, ab40658, Abcam, 1:50); rabbit anti-Myc (ab9132, Abcam, 1:1000); mouse anti-FLAG (M2, F3165, Sigma-Aldrich, 1:1000); rabbit anti-AQP1 (AB2219, Merck, 1:1000).

All antibodies have been previously validated and were subjected to additional controls. The ac-tub antibody has been used widely in the field and recognizes multiciliated cells that are absent in *Gemc1*-deficient mice (Terré et al., 2016). The AQP1 and vimentin antibodies have been validated in knockouts and extensively in publications (see Merck and Abcam, respectively). The TP73 antibody was validated in knockout animals (Marshall et al., 2016) and the signal is in the expected cell types and correlates with the mRNA level in our experiments. The vinculin antibody recognizes a band of the correct size and was used as a loading control. Myc and FLAG epitope antibodies have been validated extensively and recognize proteins of the correct size only when tagged complementary DNAs (cDNAs) are expressed. SCP1/3, γH2AX, FOXJ1 and pH3S10 antibodies (Table S1) have been validated (see manufacturer or CiteAb.com) and we have previously reported their use for meiotic staging or testes characterization (Marjanović et al., 2015).

Microscopy

Histological sections from testes, epididymis and EDs were imaged using the digital slide scanner Nanozoomer 2.0HT (Hamamatsu) and analyzed using the NDP.view2 free software (Hamamatsu). Image analysis and quantification of IHC were performed with the TMARKER free software (GitHub). For quantitation of percentage of lumen space, tubule area and lumen area were analyzed for ten tubules of PAS-stained sections (two sections per animal). The length of cytoplasmic SC arms was determined in µm using vimentin staining. Vimentin marks intermediate filaments that are seen as cytoplasmic arms surrounding the nucleus and extending from the basal region towards the tubular lumen. SC arm length was calculated in ten tubules of vimentin-stained sections (two sections per animal). Vimentin was also used to detect SC-only tubules, characterized by intense staining of the entire seminiferous tubule combined with the lack of or dramatic decrease in the number of germ cells.

Real-time quantitative PCR (RT-qPCR)

Testes, epididymis, EDs or pituitary gland were carefully dissected and collected on ice, washed in PBS and frozen. Testes were disrupted in Tri-Reagent (Sigma-Aldrich) using zirconium beads in a mechanical tissue disruptor (Precellys 24, Bertin Instruments). Total RNA was isolated according to the manufacturer's recommendations (PureLink RNA Mini Kit, Ambion) and 1 µg of RNA was treated with DNase I (Thermo Fisher Scientific) before cDNA synthesis. cDNA was generated using 0.5-1 µg of total RNA and a High Capacity RNA-to-cDNA Kit (Applied Biosystems). RT-qPCR was performed using the comparative CT method and a StepOne Real-Time PCR System (Applied Biosystems). Amplification was performed using Power SYBR Green PCR Master Mix (Applied Biosystems) or TaqMan Universal PCR Master Mix (Applied Biosystems). All assays were performed in duplicate. For TaqMan assays, *ActB* (mouse and human) probe was used as an endogenous control for normalization and a specific Taqman probe was used for mouse or human *Gemc1* (Mm02581229_m1), *Mcidas* (Mm01308202_m1), *Ccno* (Mm01297259_m1), *Foxj1* (Mm01267279_m1), *Trp73* (Mm00660220_m1) and *TP73* (Hs01056231_m1). Primers used for SYBR Green assays (Sigma-Aldrich) were *mCdc20b*_FW (5′-TATCTTAGGAGATTCAGCGG-3′) and *mCdc20b*_RV (5′-ATGTATACAGAGGTTCCGAG-3′). See also Table S2.

Development (2019) 146, dev162628. doi:10.1242/dev.162628

Germ cell isolation for FACS

Testes from adult male mice were isolated, decapsulated and processed together in a 15 ml falcon tube. Testes were first digested in EKRB medium [120 mM NaCl, 4.8 mM KCl, 25.2 mM $NaHCO_3$, 1.2 mM KH_2PO_2, 1.2 mM $MgSO_4$, 1.3 mM $CaCl_2$, 11 mM glucose, non-essential amino acids (Invitrogen), penicillin-streptomycin (Invitrogen)] with collagenase (0.5 mg/ml, Sigma-Aldrich, T6763) in a shaking water bath at 32°C for 10 min. Seminiferous tubules were allowed to sediment by gravity for 1-3 min and washed twice with EKRB. The tubules were further dissociated in EKRB with trypsin (1 mg/ml, Sigma-Aldrich, T6763) and DNase (5 µg/ml, Sigma-Aldrich, D4263) under shaking at 32°C for 15 min. Cells were resuspended thoroughly using a pipette until a single cell suspension was obtained and 1 ml of fetal bovine serum (FBS) was added to neutralize the trypsin. The cell suspension was filtered with a 70 µm cell strainer and total cell number was counted using the Neubauer chamber. One million cells/ml were resuspended in EKRB supplemented with 10% FBS and Hoechst 33342 (10 µg/ml, Life Technologies) under shaking at 32°C for 30-60 min. Propidium iodide (PI, 30 µg/ml, Life Technologies) was added to identify dead cells. Flow cytometric experiments were carried out using a FacsAria I SORP cell sorter (Beckton Dickinson), using a 70-micron nozzle at 60 PSI. Excitation of the sample was carried out using a blue (488 nm) laser for forward scatter (FSC) parameter, a green-orange laser (561 nm) was used for the excitation of PI and side scatter (SSC) signal, and a UV laser (350 nm) was used for Hoechst 33342 excitation. Cells were gated according to their scatter (FSC versus SSC) parameters; fluorescence of Hoechst 33342 was measured on live (not stained with PI) non-aggregated cells. Red emission (660/40 nm) versus blue emission (395/25 nm) from the UV laser was used on a dot plot in order to discriminate populations. Results were analyzed using the FlowJo software.

Immunofluorescence

Slides containing meiotic squashes were washed three times in PBS followed by washing in PBS-T (0.4% Triton X-100 in PBS) and blocked with 5% goat serum and 1% BSA in PBS-T for 1 h. Slides were incubated overnight at 4°C with primary antibody, washed three times in PBS-T and stained with Alexa Fluor-conjugated antibodies (594, A-11032 and A-11037; 488, A-11029 and A-11034, Life Technologies, 1:200) for 1 h at RT. After the final wash, DNA was counterstained with DAPI. Slides were mounted using Vectashield Antifade reagent (Vector Laboratories) and imaged using a Leica TCS SP5 confocal microscope equipped with 63× NA 1.40 oil immersion objective and HyD detectors. For paraffin sections, heat-induced epitope retrieval was performed in a Rodent Decloaker (Biocare Medical). Tissue sections were blocked with 10% normal sera in PBS-0.1% Triton X-100 for 1 h at RT. After three washes with PBS, tissue sections were sequentially probed with primary antibodies and fluorescently labeled secondary antibodies (Jackson ImmunoResearch).

Cell culture, transfection and western blotting

AD293 cells (Stratagene) were cultured in Dulbecco's Modified Eagle Medium (Gibco) with 10% FBS (Hyclone) and routinely tested for mycoplasma and found negative. For transient transfections, AD293 cells were seeded in 10 cm plates at 70% confluence and 10 µg of plasmid were transfected with polyethylenimine (Polysciences) the day after. The medium was changed 12 h post-transfection and cells were collected 48 h after with RIPA buffer [50 mM Tris-HCl (pH 8), 150 mM NaCl, 1% NP-40, 0.1% SDS, 0.5% sodium deoxycholate]. For tissue samples, testes were disrupted in RIPA buffer using zirconium beads in a mechanical tissue disruptor (Precellys 24). Samples were incubated for 20 min on ice and sonicated using a Bioruptor XL sonication device (Diagenode) for 15 min with 15 s intervals and centrifuged at 4°C for 20 min at 1300 rpm.

DNA constructs

The expression construct for FLAG-tagged human *GEMC1* (pcDNA5-FRT/TO-flag-hGemc1) was previously described in Terré et al. (2016). Human *CCNO* (hCCNO) cDNA was obtained from Expressed Sequence Tag EST IMAGE: 6421733 (GenBank accession number BQ917277.1) as a template and amplified using 5′-GCGAATTCCATGGTGACCCCCTGT-CCCACCAGCC-3′ and 5′-GCTCTAGATTATTTCGAGCTCGGGGGC-AGG-3′ primers. hCCNO cDNA was cloned into the pBluescript (I) SK(+) vector (Stratagene) at the EcoRI and XbaI restriction sites and then into the mammalian expression vector pCDNA3.1 (Invitrogen) modified with an N-terminal myc-tag to produce proteins N-terminally fused to myc under the control of the constitutive CMV promoter (pcDNA3.1-myc-hCcno). The pCMX-flag plasmid was used as an empty-vector control (gift from Ron Evans, the Salk Institute for Biological Studies, USA).

Meiotic squashes

Spermatocyte squashes were performed as previously described (Marjanović et al., 2015). In brief, tubules from adult mice were placed in fixative solution (2% formaldehyde, 0.05% Triton X-100 in PBS) for 10 min. To release spermatocytes from tubules, a small aliquot of the tubules was minced with tweezers on a glass slide pre-treated with poly-L lysine. Cells were covered with a coverslip and gently squashed by applying pressure with the thumb. The slide was snap-frozen in liquid nitrogen, the coverslip was removed and the slide was processed for immunofluorescence.

Acknowledgements

We thank M. Lize, H. Omran, J. Wallmeier and R. Hess for discussing unpublished data and experimental suggestions; M. Di Giacomo and Ignasi Roig for technical input; A. Nebreda, X. Salvatella and E. Batlle for reagents; L. Palenzuela for mouse colony management; the Institute for Research in Biomedicine (IRB) Barcelona histopathology facility and the Advanced Molecular Pathology Laboratory of the Institute of Molecular and Cell Biology, Singapore, for assistance with IHC and protocol establishment; and O. Reina of the IRB Biostatistics facility for help with data analysis.

Competing interests

The authors declare no competing or financial interests.

Author contributions

Conceptualization: B.T., G.G.-G., T.H.S.; Validation: B.T., M.L., G.G.-G.; Formal analysis: B.T., M.L., T.H.S.; Investigation: B.T., M.L., G.G.-G., Z.H., H.L., M.A., N.P., S.R., H.Z., T.H.S.; Resources: S.R., H.Z.; Data curation: T.H.S.; Writing - original draft: B.T., T.H.S.; Writing - review & editing: B.T., G.G.-G., N.P., S.R., T.H.S.; Visualization: B.T., T.H.S.; Supervision: T.H.S.; Project administration: B.T., T.H.S.; Funding acquisition: G.G.-G., S.R., H.Z., T.H.S.

Funding

T.H.S. was funded by the Ministerio de Economıá y Competitividad (MINECO) (BFU2015-68354/GENPATH, GINDATA and FEDER), the Centres of Excellence Severo Ochoa award and the CERCA Programme. B.T. and M.L. were supported by Severo Ochoa FPI fellowships (MINECO). G.G.-G. was supported by the Instituto de Salud Carlos III (PI13/00864) and funds from the European Regional Development Fund. H.Z. was supported by the New York Institute of Technology and the National Cancer Institute (R01CA220551). S.R. was supported by the Agency for Science, Technology and Research of Singapore. Deposited in PMC for release after 12 months.

Supplementary information

Supplementary information available online at
http://dev.biologists.org/lookup/doi/10.1242/dev.162628.supplemental

References

Abe, K. and Takano, H. (1988). Changes in distribution and staining reactivity of PAS-positive material in the mouse epididymal duct after efferent duct ligation. *Arch. Histol. Cytol.* **51**, 433-441. doi:10.1679/aohc.51.433

Al Jord, A., Shihavuddin, A., Servignat d'Aout, R., Faucourt, M., Genovesio, A., Karaiskou, A., Sobczak-Thépot, J., Spassky, N. and Meunier, A. (2017). Calibrated mitotic oscillator drives motile ciliogenesis. *Science* **358**, 803-806. doi:10.1126/science.aan8311

Amirav, I., Wallmeier, J., Loges, N. T., Menchen, T., Pennekamp, P., Mussaffi, H., Abitbul, R., Avital, A., Bentur, L., Dougherty, G. W. et al. (2016). Systematic analysis of CCNO variants in a defined population: implications for clinical phenotype and differential diagnosis. *Hum. Mutat.* **37**, 396-405. doi:10.1002/humu.22957

Arbi, M., Pefani, D. E., Kyrousi, C., Lalioti, M. E., Kalogeropoulou, A., Papanastasiou, A. D., Taraviras, S. and Lygerou, Z. (2016). GemC1 controls multiciliogenesis in the airway epithelium. *EMBO Rep.* **17**, 400-413. doi:10.15252/embr.201540882

Aumüller, G., Steinbrück, M., Krause, W. and Wagner, H.-J. (1988). Distribution of vimentin-type intermediate filaments in Sertoli cells of the human testis, normal and pathologic. *Anat. Embryol. (Berl)* **178**, 129-136. doi:10.1007/BF02463646

Balestrini, A., Cosentino, C., Errico, A., Garner, E. and Costanzo, V. (2010). GEMC1 is a TopBP1-interacting protein required for chromosomal DNA replication. *Nat. Cell Biol.* **12**, 484-491. doi:10.1038/ncb2050

Boon, M., Wallmeier, J., Ma, L., Loges, N. T., Jaspers, M., Olbrich, H., Dougherty, G. W., Raidt, J., Werner, C., Amirav, I. et al. (2014). MCIDAS mutations result in a mucociliary clearance disorder with reduced generation of multiple motile cilia. *Nat. Commun.* **5**, 4418. doi:10.1038/ncomms5418

Chen, J., Knowles, H. J., Hebert, J. L. and Hackett, B. P. (1998). Mutation of the mouse hepatocyte nuclear factor/forkhead homologue 4 gene results in an absence of cilia and random left-right asymmetry. *J. Clin. Invest.* **102**, 1077-1082. doi:10.1172/JCI4786

Chong, Y. L., Zhang, Y., Zhou, F. and Roy, S. (2018). Distinct requirements of E2f4 versus E2f5 activity for multiciliated cell development in the zebrafish embryo. *Dev. Biol.* **443**, 165-172. doi:10.1016/j.ydbio.2018.09.013

Chung, M.-I., Peyrot, S. M., LeBoeuf, S., Park, T. J., McGary, K. L., Marcotte, E. M. and Wallingford, J. B. (2012). RFX2 is broadly required for ciliogenesis during vertebrate development. *Dev. Biol.* **363**, 155-165. doi:10.1016/j.ydbio.2011.12.029

Clulow, J., Jones, R. C., Hansen, L. A. and Man, S. Y. (1998). Fluid and electrolyte reabsorption in the ductuli efferentes testis. *J. Reprod. Fertil. Suppl.* **53**, 1-14.

Comazzetto, S., Di Giacomo, M., Rasmussen, K. D., Much, C., Azzi, C., Perlas, E., Morgan, M. and O'Carroll, D. (2014). Oligoasthenoteratozoospermia and infertility in mice deficient for miR-34b/c and miR-449 loci. *PLoS Genet.* **10**, e1004597. doi:10.1371/journal.pgen.1004597

Danielian, P. S., Bender Kim, C. F., Caron, A. M., Vasile, E., Bronson, R. T. and Lees, J. A. (2007). E2f4 is required for normal development of the airway epithelium. *Dev. Biol.* **305**, 564-576. doi:10.1016/j.ydbio.2007.02.037

Danielian, P. S., Hess, R. A. and Lees, J. A. (2016). E2f4 and E2f5 are essential for the development of the male reproductive system. *Cell Cycle* **15**, 250-260. doi:10.1080/15384101.2015.1121350

Didon, L., Zwick, R. K., Chao, I. W., Walters, M. S., Wang, R., Hackett, N. R. and Crystal, R. G. (2013). RFX3 modulation of FOXJ1 regulation of cilia genes in the human airway epithelium. *Respir. Res.* **14**, 70. doi:10.1186/1465-9921-14-70

El Zein, L., Ait-Lounis, A., Morle, L., Thomas, J., Chhin, B., Spassky, N., Reith, W. and Durand, B. (2009). RFX3 governs growth and beating efficiency of motile cilia in mouse and controls the expression of genes involved in human ciliopathies. *J. Cell Sci.* **122**, 3180-3189. doi:10.1242/jcs.048348

Funk, M. C., Bera, A. N., Menchen, T., Kuales, G., Thriene, K., Lienkamp, S. S., Dengjel, J., Omran, H., Frank, M. and Arnold, S. J. (2015). Cyclin O (Ccno) functions during deuterosome-mediated centriole amplification of multiciliated cells. *EMBO J.* **34**, 1078-1089. doi:10.15252/embj.201490805

Holembowski, L., Kramer, D., Riedel, D., Sordella, R., Nemajerova, A., Dobbelstein, M. and Moll, U. M. (2014). TAp73 is essential for germ cell adhesion and maturation in testis. *J. Cell Biol.* **204**, 1173-1190. doi:10.1083/jcb.201306066

Inoue, S., Tomasini, R., Rufini, A., Elia, A. J., Agostini, M., Amelio, I., Cescon, D., Dinsdale, D., Zhou, L., Harris, I. S. et al. (2014). TAp73 is required for spermatogenesis and the maintenance of male fertility. *Proc. Natl. Acad. Sci. USA* **111**, 1843-1848. doi:10.1073/pnas.1323416111

Joseph, A., Shur, B. D. and Hess, R. A. (2011). Estrogen, efferent ductules, and the epididymis. *Biol. Reprod.* **84**, 207-217. doi:10.1095/biolreprod.110.087353

Kyrousi, C., Arbi, M., Pilz, G.-A., Pefani, D.-E., Lalioti, M.-E., Ninkovic, J., Gotz, M., Lygerou, Z. and Taraviras, S. (2015). Mcidas and GemC1 are key regulators for the generation of multiciliated ependymal cells in the adult neurogenic niche. *Development* **142**, 3661-3674. doi:10.1242/dev.126342

Lafkas, D., Shelton, A., Chiu, C., de Leon Boenig, G., Chen, Y., Stawicki, S. S., Siltanen, C., Reichelt, M., Zhou, M., Wu, X. et al. (2015). Therapeutic antibodies reveal Notch control of transdifferentiation in the adult lung. *Nature* **528**, 127-131. doi:10.1038/nature15715

Lu, H., Anujan, P., Zhou, F., Zhang, Y., Chong, Y. L., Bingle, C. D. and Roy, S. (2019). Mcidas mutant mice reveal a two-step process for the specification and differentiation of multiciliated cells in mammals. *Development* **46**, dev172643. doi:10.1242/dev.172643

Ma, L., Quigley, I., Omran, H. and Kintner, C. (2014). Multicilin drives centriole biogenesis via E2f proteins. *Genes Dev.* **28**, 1461-1471. doi:10.1101/gad.243832.114

Marcet, B., Chevalier, B., Luxardi, G., Coraux, C., Zaragosi, L. E., Cibois, M., Robbe-Sermesant, K., Jolly, T., Cardinaud, B., Moreilhon, C. et al. (2011). Control of vertebrate multiciliogenesis by miR-449 through direct repression of the Delta/Notch pathway. *Nat. Cell Biol.* **13**, 693-699. doi:10.1038/ncb2241

Marjanović, M., Sánchez-Huertas, C., Terré, B., Gómez, R., Scheel, J. F., Pacheco, S., Knobel, P. A., Martínez-Marchal, A., Aivio, S., Palenzuela, L. et al. (2015). CEP63 deficiency promotes p53-dependent microcephaly and reveals a role for the centrosome in meiotic recombination. *Nat. Commun.* **6**, 7676. doi:10.1038/ncomms8676

Marshall, C. B., Mays, D. J., Beeler, J. S., Rosenbluth, J. M., Boyd, K. L., Santos Guasch, G. L., Shaver, T. M., Tang, L. J., Liu, Q., Shyr, Y. et al. (2016). p73 is required for multiciliogenesis and regulates the Foxj1-associated gene network. *Cell Rep.* **14**, 2289-2300. doi:10.1016/j.celrep.2016.02.035

Nemajerova, A., Kramer, D., Siller, S. S., Herr, C., Shomroni, O., Pena, T., Gallinas Suazo, C., Glaser, K., Wildung, M., Steffen, H. et al. (2016). TAp73 is a central transcriptional regulator of airway multiciliogenesis. *Genes Dev.* **30**, 1300-1312. doi:10.1101/gad.279836.116

Núnez-Ollé, M., Jung, C., Terré, B., Balsiger, N. A., Plata, C., Roset, R., Pardo-Pastor, C., Garrido, M., Rojas, S., Alameda, F. et al. (2017). Constitutive Cyclin O deficiency results in penetrant hydrocephalus, impaired growth and infertility. *Oncotarget* **8**, 99261-99273. doi:10.18632/oncotarget.21818

Pan, J.-H., Adair-Kirk, T. L., Patel, A. C., Huang, T., Yozamp, N. S., Xu, J., Reddy, E. P., Byers, D. E., Pierce, R. A., Holtzman, M. J. et al. (2014). Myb permits multilineage airway epithelial cell differentiation. *Stem Cells* **32**, 3245-3256. doi:10.1002/stem.1814

Roig, M. B., Roset, R., Ortet, L., Balsiger, N. A., Anfosso, A., Cabellos, L., Garrido, M., Alameda, F., Brady, H. J. M. and Gil-Gómez, G. (2009). Identification of a novel cyclin required for the intrinsic apoptosis pathway in lymphoid cells. *Cell Death Differ.* **16**, 230-243. doi:10.1038/cdd.2008.145

Song, R., Walentek, P., Sponer, N., Klimke, A., Lee, J. S., Dixon, G., Harland, R., Wan, Y., Lishko, P., Lize, M. et al. (2014). miR-34/449 miRNAs are required for motile ciliogenesis by repressing cp110. *Nature* **510**, 115-120. doi:10.1038/nature13413

Stubbs, J. L., Vladar, E. K., Axelrod, J. D. and Kintner, C. (2012). Multicilin promotes centriole assembly and ciliogenesis during multiciliate cell differentiation. *Nat. Cell Biol.* **14**, 140-147. doi:10.1038/ncb2406

Tan, F. E., Vladar, E. K., Ma, L., Fuentealba, L. C., Hoh, R., Espinoza, F. H., Axelrod, J. D., Alvarez-Buylla, A., Stearns, T., Kintner, C. et al. (2013). Myb promotes centriole amplification and later steps of the multiciliogenesis program. *Development* **140**, 4277-4286. doi:10.1242/dev.094102

Terré, B., Piergiovanni, G., Segura-Bayona, S., Gil-Gómez, G., Youssef, S. A., Attolini, C. S., Wilsch-Bräuninger, M., Jung, C., Rojas, A. M., Marjanović, M. et al. (2016). GEMC1 is a critical regulator of multiciliated cell differentiation. *EMBO J.* **35**, 942-960. doi:10.15252/embj.201592821

Tomasini, R., Tsuchihara, K., Wilhelm, M., Fujitani, M., Rufini, A., Cheung, C. C., Khan, F., Itie-Youten, A., Wakeham, A., Tsao, M. S. et al. (2008). TAp73 knockout shows genomic instability with infertility and tumor suppressor functions. *Genes Dev.* **22**, 2677-2691. doi:10.1101/gad.1695308

Tsao, P. N., Vasconcelos, M., Izvolsky, K. I., Qian, J., Lu, J. and Cardoso, W. V. (2009). Notch signaling controls the balance of ciliated and secretory cell fates in developing airways. *Development* **136**, 2297-2307. doi:10.1242/dev.034884

Vladar, E. K., Stratton, M. B., Saal, M. L., Salazar-De Simone, G., Wang, X., Wolgemuth, D., Stearns, T. and Axelrod, J. D. (2018). Cyclin-dependent kinase control of motile ciliogenesis. *eLife* **7**, e36375. doi:10.7554/eLife.36375

Wallmeier, J., Al-Mutairi, D. A., Chen, C. T., Loges, N. T., Pennekamp, P., Menchen, T., Ma, L., Shamseldin, H. E., Olbrich, H., Dougherty, G. W. et al. (2014). Mutations in CCNO result in congenital mucociliary clearance disorder with reduced generation of multiple motile cilia. *Nat. Genet.* **46**, 646-651. doi:10.1038/ng.2961

Wu, J., Bao, J., Kim, M., Yuan, S., Tang, C., Zheng, H., Mastick, G. S., Xu, C. and Yan, W. (2014). Two miRNA clusters, miR-34b/c and miR-449, are essential for normal brain development, motile ciliogenesis, and spermatogenesis. *Proc. Natl. Acad. Sci. USA* **111**, E2851-E2857. doi:10.1073/pnas.1407777111

You, Y., Huang, T., Richer, E. J., Schmidt, J.-E. H., Zabner, J., Borok, Z. and Brody, S. L. (2004). Role of f-box factor foxj1 in differentiation of ciliated airway epithelial cells. *Am. J. Physiol. Lung Cell. Mol. Physiol.* **286**, L650-L657. doi:10.1152/ajplung.00170.2003

Yu, X., Ng, C. P., Habacher, H. and Roy, S. (2008). Foxj1 transcription factors are master regulators of the motile ciliogenic program. *Nat. Genet.* **40**, 1445-1453. doi:10.1038/ng.263

Yuan, S., Tang, C., Zhang, Y., Wu, J., Bao, J., Zheng, H., Xu, C. and Yan, W. (2015). mir-34b/c and mir-449a/b/c are required for spermatogenesis, but not for the first cleavage division in mice. *Biol. Open* **4**, 212-223. doi:10.1242/bio.201410959

Yuan, S., Liu, Y., Peng, H., Tang, C., Hennig, G. W., Wang, Z., Wang, L., Yu, T., Klukovich, R., Zhang, Y. et al. (2019). Motile cilia of the male reproductive system require miR-34/miR-449 for development and function to generate luminal turbulence. *Proc. Natl. Acad. Sci. USA* **116**, 3584-3593. doi:10.1073/pnas.1817018116

Zhou, F., Narasimhan, V., Shboul, M., Chong, Y. L., Reversade, B. and Roy, S. (2015). Gmnc is a master regulator of the multiciliated cell differentiation program. *Curr. Biol.* **25**, 3267-3273. doi:10.1016/j.cub.2015.10.062